Network-Constrained Transactive Control for Multi-Microgrids-based Distribution Networks with Soft Open Points

Xiaodong Yang, *Member, IEEE,* Zehao Song, Jinyu Wen, *Member, IEEE,* Lijian Ding, Menglin Zhang, Qiuwei Wu, *Senior Member, IEEE,* and Shijie Cheng, *Life Fellow, IEEE*

***Abstract*—Different from most transactive control studies only focusing on economic aspect, this paper develops a novel network-constrained transactive control (NTC) framework that can address both economic and secure issues for a multi-microgrids-based distribution network considering uncertainties. In particular, we innovatively integrate a transactive energy market with the novel power-electronics device (i.e., soft open point) based AC power flow regulation technique to improve economic benefits for each individual microgrid and meanwhile ensure the voltage security of the entire distribution network. In this framework, a dynamic two-timescale NTC model consisting of slow-timescale pre-scheduling and real-time corrective scheduling stages is formulated to work against multiple system uncertainties. Moreover, the original bilevel game problems are transformed into a single-level mixed-integer second-order cone programming problem through KKT conditions, duality, linearization and relaxation techniques to avoid iterations of transitional methods, so as to improve the solving efficiency. Finally, numerical simulations on modified 33-bus and 123-bus test systems with multi-microgrids verify the effectiveness of the proposed framework.**

***Index Terms*—Transactive control, multi-microgrids, soft open point, transactive energy market, network-constrained**

I. INTRODUCTION

DISTRIBUTION networks (DNs) are undergoing a transition from traditional passive systems to active ones due to the increasing promotion of distributed generations, active flexible resources as well as the information and control technologies [1]. In this context, with the integration of high-penetration renewable energy sources (RESs), prosumers and various kinds of energy storages, microgrids (MGs) have been emerged as promising self-managed subsystems in DNs for efficient consumption of localized renewable power [2]. Recently, multi-microgrids (MMGs) are considered as an emerging network designed to further enhance the benefits of MGs [3]. The operation and reliability of the system can be improved by connecting multiple MGs to make a DN with multi-microgrids. Thus, MMGs will be an important network feature in the future DNs, with the merit of operational cost savings [4], transmission losses reduction [5], increased utilization efficiency of flexible resources [6], accommodating more RESs and resilience enhancement [7], [8].

Extensive studies have focused on the energy scheduling of MMG systems, which can be classified into two categories: direct control-based and local energy market-based methods. The control-based methods [9]–[11] are designed from the point of view of the distribution network operator (DNO) or aggregator to determine direct control commands for all controllable parts by collecting all the information from MGs. Although this kind of methods are easy to be implemented, there still have many drawbacks such as privacy concerns, low scalability and also limits the autonomy of individual MGs.

To tackle them, local energy market-based methods emerge for enabling decentralized cooperation among the autonomous MGs, such as, multiagent-based [12], game theory-based [4], [13], [14], auction theory-based [15] methods, and semi-market-based method under supervision [16].

Compared to the direct control-based methods, local energy market-based methods tend to provide market platforms that enable the exchange of energy between the participants only with limited amount of private information exchanges [16], which protect self-interests of autonomous MGs and have good scalability. Nevertheless, above mentioned works only focused on active power optimization for economic operation of MMG systems, while concerning little about the joint investigation of the economic issues of MMG scheduling and the technical issues of DN operation. That is, the distribution network constraints are ignored in [12], [14]–[17].

Economic and secure operation issues are two major concerns of the operators of DNs with MMGs. In practice, the decision-makings of multiple MGs will have an impact on the DN operation, which would affect the energy scheduling of individual MGs conversely if the network constraints including line/transformer capacity and voltage/current limitations are fully considered [18]. Any non-coordination method may lead to the over-utilized of grid assets and may realize suboptimal performances on voltage profiles and overall operational economy. Meanwhile, the inherent volatility and intermittency of RESs will lead to frequent fluctuation of feeder power, thus resulting in voltage sharp fluctuation and even violations [19]. In addition, the uneven between power generations and consumptions is further aggravated due to the centralized power consumption in certain nodes, which leads to the power imbalance between feeders [20], thus disturbing the power flow and increasing system power losses [21]. Consequently,

This work was supported in part by the National Natural Science Foundation of China under Grant 52007074, in part by the Joint Fund of National Natural Science Foundation of China under Grants U22B20116 and U19A20106, and in part by the Institute of Energy, Hefei Comprehensive National Science Center, under Grant 19KZS207. (*Corresponding author: Jinyu Wen; Lijian Ding.*)

X. Yang and L. Ding are with School of Electric Engineering and Automation, Hefei University of Technology, Hefei 230009, China (e-mail: yang_xd90@163.com; ljding@hfut.edu.cn).

J. Wen and S. Cheng are with State Key Laboratory of Advanced Electromagnetic Engineering and Technology, School of Electrical and Electronic Engineering, Huazhong University of Science and Technology, Wuhan, 430074, China (e-mail: jinyu.wen@hust.edu.cn; sjcheng@hust.edu.cn).

Q. Wu and Z. Song are with the Tsinghua-Berkeley Shenzhen Institute, Tsinghua Shenzhen International Graduate School, Tsinghua University, Shenzhen 518055, China (e-mail: qiuwu@sz.tsinghua.edu.cn; songzh22@mails.tsinghua.edu.cn).

M. Zhang is with the School of Automation, China University of Geosciences, Wuhan, 430074, China (e-mail: zhangmenglin@cug.edu.cn).

these consequences are required to be addressed when optimal managing the DN with MMGs.

Fortunately, transactive control (TC) is emerging as one of the most promising solutions for respecting all the participants' interests [22], including MG owners and DNO. Transactive control refers to a set of mechanisms for the coordination of various participants through value exchanges, where the price signals are applied to bridge all the components in the system, and the agreement between the control decisions of different components are determined via transactions [23]. Liu *et al.* [23] proposed a transactive energy based method for the coordinated operation of networked MGs and DNO with distributionally robust optimization. Yan *et al.* [24] presented a two-level network-constrained method that guarantees the optimal topology of DN and the transactive energy trading among the MMGs. However, careful review of these excellent studies reveals that the limitation still exists, i.e., the system uncertainties posed by RESs and load demands are not properly addressed. In this regard, any prediction error will lead to inappropriate control commands to physical components, which is undoubtedly detrimental to economic optimality and may even raise security issues to the DN system.

In addition, earlier network-constrained transactive control studies mainly focused on the MG resources management and market clearing algorithms and only took the network security constraints into consideration, where the active measures to further optimize the DN are ignored. In view of this, [18] and [24] proposed to use network reconfiguration to change the topology of the DN for power flow adjustment, which could reduce power losses and mitigate voltage violations. However, limited by the action frequency of line/tie switches, there still has space for performance improvement. To improve this, soft open point (SOP), a novel fully-controlled power-electronics device enabling the flexible connection between feeders, is introduced to enhance the flexibility of DN system operations [25]. The SOPs can realize accurately and continuously active/reactive power regulation of the connected feeders and has rapid response speed [1], [21], which have been proved more effective than network reconfiguration in power flow adjustment [26]. Still, the application of SOPs in transactive energy field has not been sufficiently studied previously.

Motivated by aforementioned facts, this paper aims to develop a network-constrained transactive control (NTC) framework for an MMGs-based DN system with SOPs under an uncertain environment. This framework organizes a local transactive energy market for both MG owners and DNO to participate in, and respects the interests and preference of individual MGs, and takes active measures to optimize the DN operation to ensure its security. To our knowledge, we are among the first to explore the benefits of power-electronics device (i.e., SOP) in the network-constrained coordination between the MMGs and DNO, and also address the system uncertainties.

The salient features of this paper are reflected in Table I through the comparison with existing works, and our major contributions are threefold:

TABLE I
COMPARATIVE FEATURES OF PREVIOUS STUDIES

Reference	Transactive market	Network constraints	System uncertainty	Active measures of the DN
[11], [27]	–	–	Yes	–
[23]	Yes	Yes	–	–
[18], [24]	Yes	Yes	–	Yes (network reconfiguration)
Proposed NTC	Yes	Yes	Yes	Yes (using SOPs)

- *Formulating a network-constrained transactive control framework to ensure secure-economic operation with the use of SOPs.* Unlike most TC works [22], [23] only focusing on economic aspect and different from existing Volt/Var control methods [1], [19] that do not consider the energy interactions of demand-side entities, a network-constrained transactive control framework that can address both economic and secure issues for an MMGs-based distribution network simultaneously is formulated in this work. The active measure of introducing SOPs is innovatively integrated with the AC optimal power flow technique, which could improve economic benefits to the MGs and meanwhile ensure the voltage security and reduce the power losses of the DN, this has not been studied before.
- *Presenting an efficient way for coordinating multiple entities in DNs under uncertainties.* Different financial entities, i.e., distribution network operator and microgrids, are coordinated by a dynamic two-timescale NTC model, which consists of slow-timescale pre-scheduling and real-time scheduling to work against multiple system uncertainties. This price-bridged coordination is conducive to the flexibility provision of demand side resources, and also can help to regulate the system power flow to improve the utilization of renewable energy. Furthermore, most decentralized market-based methods clear the prices or make the decisions via iterative algorithms. In contrast, we transform the bilevel game problem into a single-level mixed integer second order cone programming (MISOCP) problem through KKT conditions, duality, linearization and relaxation techniques, which is beneficial to the improvement of solving efficiency.

The remainder of this paper is organized as follows: Section II presents the problem description of the DN with MMGs, and outlines the proposed NTC framework. Section III introduces the optimization models of the DNO and individual MGs, the problem transformation is also given. Detailed formulations of proposed NTC and solution methodology are presented in Section IV. Section V provides the numerical simulations and Section VI concludes this work.

II. PROPOSED TRANSACTIVE CONTROL FRAMEWORK

In this study, we consider a common system architecture for a distribution network with MMGs. The distribution network is divided into several MG areas, and is connected to the upstream high voltage (HV) system. In an MG, RESs (mainly the photovoltaic array (PV) and wind turbine (WT)), energy storage system (ESS), general loads and controllable loads are included. Besides, the fully controlled power-electronic devices, *i.e.*, SOPs, are installed in the DN for accurately power flow regulation. Both the DNO and MG owners are considered as individual entities in the system and determines its own operation decisions for its controllable resources. Each MG owner determines the consumption plan of controllable loads, the charing/discharging power of ESS and the exchange power series with the DN to minimize its operational cost. The exchange power represents the imbalance between the demand and generation inside a microgrid that will be compensated by the distribution system with the payment according to clearing price λ_t. At the same time, the DN operator determines the

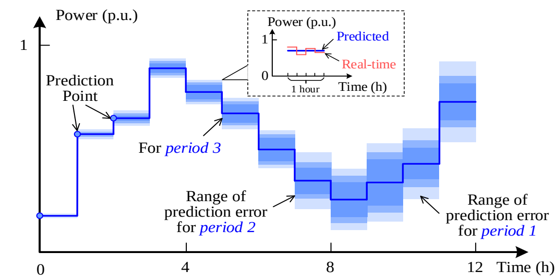

Fig. 1. Sketch view of prediction errors in different time periods.

clearing pricing with the MGs and the active/reactive power outputs of SOPs to improve its operation quality perspective from both economy and security.

In view of the above, since the operation of the DNO and each MG is correlated with each other, their operation need to be coordinated in order to achieve the efficient operation of the entire system. In this case, a transactive control based framework is designed for the coordination of the DN operator and MGs.

The conclusion of main properties for the focused MMGs-based DN is given as follows before designing our approach.

- The DNO acts as the leader of the DN system operation and determines the dynamic system prices for the demand and supply in the DN. The MG owners are the followers during the system operation and react to the DNO's decisions. Before the actual real-time implementation, the DNO determines the dynamic system prices and transmits them to all the MGs inside the DN, and the MGs then decide their energy schedules according to the system prices and send their decisions to the DNO. This is a typical iteration process in which the final results are obtained after several iterations.
- The high-penetration renewable energy generations are included in the DN, their uncertainties will cause the deviations between the obtained results and expected ones (as shown in Fig. 1), and may also lead to the problems of complex power flow and frequent voltage deviations or even voltage violations. As shown in Fig. 1, the prediction error of the renewable energy generations will be larger as the prediction time scale increase, e.g., the prediction error of the renewable energy generations for the time spot which is 2 hrs from current time spot is larger than that is 1 hr from current time spot. Intuitively, the prediction of the current time spot is the most accurate one.
- Lots of previous MMG studies [4], [28] only focus on the active power scheduling while ignoring network topology and active power flow reshaping of the DN. Such non-coordination between MMG and DN operations might lead to over-utilization of DN-side devices, posing the possibility of network congestion and voltage deviation.

Considering above, to balance the computational efficiency and the scheduling performances, in the remaining of this paper we focus on providing a mathematical formulation of *two-timescale* network-constrained transactive control method for MMGs-based distribution networks, with the coordination of DNO and MGs optimizations. The framework of the proposed NTC method is depicted in Fig. 2.

In the proposed NTC framework, the DNO and each MG are considered as individual entities and tend to maximize their own interests. A transacitive energy market is organized by

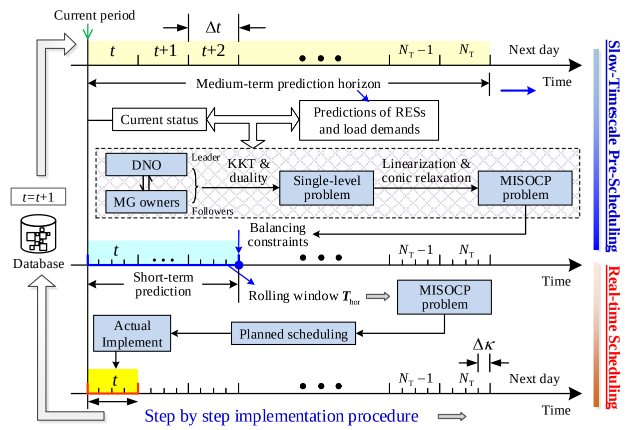

Fig. 2. Schematic illustration of the proposed two-timescale NTC method.

the DNO to coordinate the energy scheduling of the DN and MGs. As such, the energy scheduling of the DN and MGs can be coordinated according to the real-time operation conditions, and the autonomy of individual MGs can be further released and utilized. As depicted in Fig. 2, the details of the proposed NTC model are elaborated as follows:

At the slow-timescale pre-dispatching stage, the Stackelberg game between the leader DNO and the followers MGs is modeled as a bi-level optimization problem, where the upper level leader DNO determines the clearing price and the lower level followers MGs determine their net power profiles according to the clearing price. Then, based on strong duality theory and KKT conditions, the origin bi-level optimization problem can be transformed to an equivalent single-level optimization problem that can achieve the optimal solutions for both DNO and MGs, i.e., the equilibrium point of the established Stackelberg game model simultaneously. Moreover, the single-level model is further simplified to a tractable MISOCP model through linearization and second order cone relaxation techniques. Note that the predictions of RESs and load demands are day-ahead, as mentioned before in Fig. 1, the prediction error will increase as the prediction time-scale increase, thus, the pre-scheduling decisions may perform poorly in the real-time stage with the disturbance arising from the uncertainty of the RESs and load demands. Therefore, the pre-scheduling decisions can only be treated as the strategy reference for the system operator before the intra-day operation.

At the real-time corrective scheduling stage, the system first collects the short-term predictions from the current period. As we previously mentioned, the prediction error is more accurate with shorter prediction time period. Then, the DNO and MGs make their latest decisions based on the updated predictions using the constructed tractable MISOCP model. Note that the DNO and MGs only implement the current period decision to improve the accuracy of their scheduling decisions, and at next period they continue the prediction updating and current period decision implementing process till the end of the scheduling horizon. Therefore, at each operating time period the scheduling decision implemented is based on the latest prediction information, which can ensure the accuracy of the decision and thus enabling the proposed model adaptive to the unforeseen changes.

III. System Modeling and Model Transformation

In this section, the optimization models of the distribution network operator and microgrids are formulated. Moreover,

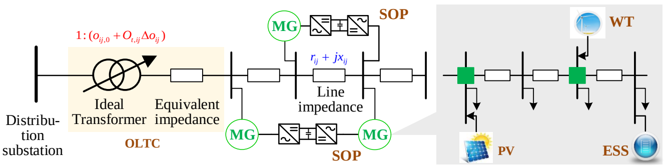

Fig. 3. Simplified model of MMGs-based distribution network with SOPs.

the equivalent transformation of the interactive bilevel problem is described in detail.

A. Optimization Model of Distribution Network Operator

The optimization model of the distribution network operator can be expressed as

$$\min \mathscr{F}_{\mathcal{D}}(\boldsymbol{x}) = \mathbb{a}_{\mathrm{o}}\left(f_{\text{Grid}} + f_{\text{loss}} + f_{\text{sw}} - \mathscr{I}_{\text{inc}}\right) + \mathbb{b}_{\mathrm{v}}\mathcal{F}_{\text{vd}} \tag{1}$$

$$\begin{cases} f_{\text{Grid}} = \sum_{t=1}^{N_T}\left(\frac{X_t - W_t}{2}|g_t| + \frac{X_t + W_t}{2}g_t\right)\Delta t; \\ f_{\text{loss}} = \mathscr{C}_{\text{loss}}\left(\sum\limits_{t=1}^{N_T}\sum\limits_{ij\in\Omega_l} r_{ij}I_{t,ij}^2\Delta t + \sum\limits_{t=1}^{N_T}\sum\limits_{i=1}^{N_N} P_{t,i}^{\text{sop,loss}}\Delta t\right); \\ f_{\text{sw}} = \sum\limits_{ij\in\Omega_O}\sum\limits_{t=1}^{N_T}(\mathscr{C}_{\text{tap}}|O_{t,ij} - O_{t-1,ij}|); \\ \mathscr{I}_{\text{inc}} = \sum\limits_{t=1}^{N_T}\sum\limits_{n=1}^{N_{\text{mg}}}\lambda_t P_{t,n}^{\text{net}}\Delta t; \\ \mathcal{F}_{\text{vd}} = \sum\limits_{t=1}^{N_T}\sum\limits_{i=1}^{N_N}\left|U_{t,i}^2 - \widetilde{U}_{\text{ref}}^2\right|. \end{cases} \tag{2}$$

Eq. (1) is a linear weighted combination of operational cost and voltage deviation minimization problems, where $\mathbb{a}_{\mathrm{o}}$ and $\mathbb{b}_{\mathrm{v}}$ are the weight coefficients which can be determined using a subjective weighting method [29]. f_{Grid}, f_{loss}, f_{sw} and $\mathscr{I}_{\text{inc}}$ are the grid cost, network losses cost, adjusting cost of on-load tap changer (OLTC), and the income from MGs, respectively. X_t and W_t are the import and export energy trading prices with HV grid, respectively; g_t is the net load of DN system, which is positive if the DN imports energy from the HV grid and is negative if the DN exports energy to the HV grid; $\mathscr{C}_{\text{loss}}$ and $\mathscr{C}_{\text{tap}}$ are the cost coefficients associated with power losses and OLTC, respectively; r_{ij} and x_{ij} are the resistance/reactance of branch ij; $I_{t,ij}$ is the current of branch ij at period t; $P_{t,i}^{\text{sop,loss}}$ is the active power losses caused by SOP at period t (see (14)); N_T, N_N, and N_{mg} are the total numbers of time periods, nodes and MGs inside the DN, respectively; Δt is the discrete time interval in slow-timescale pre-scheduling stage; Ω_l and Ω_O are the sets of all the branches and the branches with OLTCs, respectively; λ_t is the clearing price in transactive market at period t; $P_{t,n}^{\text{net}}$ represents the net load of MG n at period t. $\mathcal{F}_{\text{vd}}$ is the voltage deviations of the entire distribution network compared to the predetermined reference voltage point $\widetilde{U}_{\text{ref}}$ during the whole operation time period, which can be used to evaluate the voltage quality of the system.

The objectives of the DNO are twofold: first, to minimize the operational cost (consisting of the grid cost f_{Grid}, OLTC adjusting cost f_{sw} and the income $\mathscr{I}_{\text{inc}}$ from MGs); second, to reshape the power flow for power loss reduction and voltage regulation (represented as f_{loss} and $\mathcal{F}_{\text{vd}}$). In this process, the operational security of the DN has to be ensured. That is, the responsibility of the DNO is to operate the distribution network to improve the economy and voltage security through the active measure of regulating SOPs and negotiation with MGs.

1) Network constraints of the DN: Considering a generic and simplified radial distribution network with SOPs represented in Fig. 3 for research, in which the OLTC is equivalent to an ideal transformer connected in series with an equivalent impedance [30], and the internal microgrids are connected to each other by SOPs, which can transfer bidirectional power flexibly between networked-microgrids to promote the transactive energy sharing. Specifically, the microgrids are equipped with RESs such as WT, PV and energy storage system, the MGs can share the excessive renewable energy with other entities to improve the local renewable energy utilization. The widely used *Distflow* branch model is adopted to model the DN [29], as described in the following.

$$\sum\nolimits_{ik\in\Omega_l} P_{t,ik} - \sum\nolimits_{ji\in\Omega_l}(P_{t,ji} - r_{ji}I_{t,ji}^2) = P_{t,i}; \tag{3}$$

$$\sum\nolimits_{ik\in\Omega_l} Q_{t,ik} - \sum\nolimits_{ji\in\Omega_l}(Q_{t,ji} - x_{ji}I_{t,ji}^2) = Q_{t,i}; \tag{4}$$

$$U_{t,i}^2 - U_{t,j}^2 - 2(r_{ij}P_{t,ij} + x_{ij}Q_{t,ij}) + (r_{ij}^2 + x_{ij}^2)I_{ij}^2 = 0; \tag{5}$$

$$I_{t,ij}^2 U_{t,i}^2 = P_{t,ij}^2 + Q_{t,ij}^2; \tag{6}$$

$$P_{t,i} = P_{t,i}^{\text{p}} + P_{t,i}^{\text{w}} + P_{t,i}^{\text{sop}} - P_{t,i}^{\text{L}} + (d_{t,i}^{\text{ess}} - c_{t,i}^{\text{ess}}); \tag{7}$$

$$Q_{t,i} = Q_{t,i}^{\text{p}} + Q_{t,i}^{\text{w}} + Q_{t,i}^{\text{sop}} - Q_{t,i}^{\text{L}}; \tag{8}$$

where $P_{t,i}/Q_{t,i}$ are the sum of active/reactive power injection at node i at period t; $P_{t,ij}/Q_{t,ij}$ are the active/reactive power flow of branch ij at period t; $U_{t,i}$ is the voltage magnitude of node i at period t; $P_{t,i}^{\text{L}}$ and $Q_{t,i}^{\text{L}}$ are the active/reactive load consumptions of node i at period t, respectively; $c_{t,i}^{\text{ess}}$ and $d_{t,i}^{\text{ess}}$ are the charging/discharging power of ESS i at period t, respectively; $P_{t,i}^{\text{p}}/Q_{t,i}^{\text{p}}$ are the active/reactive power injected by PV unit at node i, with the relationship of:

$$Q_{t,i}^{\text{p}} = P_{t,i}^{\text{p}}\tan\theta_i^{\text{p}} \tag{9}$$

$$\sqrt{(P_{t,i}^{\text{p}})^2 + (Q_{t,i}^{\text{p}})^2} \leq S_i^{\text{p}} \tag{10}$$

where θ_i^{p} is the power factor angle of PV i, S_i^{p} is the capacity of PV i; and constraints (9)-(10) are also hold for WTs.

The security constraints of the studied DN are presented as:

$$\underline{U}^2 \leq U_{t,i}^2 \leq \overline{U}^2, \ \forall t, i \tag{11}$$

$$I_{t,ij}^2 \leq \overline{I}^2, \ \forall t, (i,j) \in \Omega_l \tag{12}$$

where $\overline{I}$ is the upper current limit of any branch; $\overline{U}$ and $\underline{U}$ are the upper/lower limits of statutory voltage range, respectively. Constraint (11) represents the system voltage limits, and the maximum line current capacity is shown in (12).

2) SOP operation constraints: In this work, the back-to-back voltage source converters (VSCs)-based SOP device is utilized, whose features can be found in [29]. In this regard, optimization variables of the SOP consist of the active and reactive power outputs of the two VSCs, thus its flexibility model and constraints are formulated as follows [19], [31]:

i) Active/reactive power constraints:

$$P_{t,i}^{\text{sop}} + P_{t,j}^{\text{sop}} + P_{t,i}^{\text{sop,loss}} + P_{t,j}^{\text{sop,loss}} = 0, \ \forall t, (i,j) \in \Omega_{\text{S}} \tag{13}$$

$$P_{t,i}^{\text{sop,loss}} = A_i^{\text{sop}}\sqrt{(P_{t,i}^{\text{sop}})^2 + (Q_{t,i}^{\text{sop}})^2}, \ \forall t \tag{14}$$

$$\underline{Q}_i^{\text{sop}} \leq Q_{t,i}^{\text{sop}} \leq \overline{Q}_i^{\text{sop}}, \ \forall t \tag{15}$$

ii) Capacity constraints:

$$\sqrt{(P_{t,i}^{\text{sop}})^2 + (Q_{t,i}^{\text{sop}})^2} \leq S_i^{\text{sop}}, \ \forall t \tag{16}$$

where $P_{t,i}^{\text{sop}}/Q_{t,i}^{\text{sop}}$ are active/reactive power injection by VSC at node i at period t; Ω_{S} is the set of branches with SOPs; S_i^{sop}

is the capacity of VSC at node i; $\underline{Q}_i^{\rm sop}$ and $\overline{Q}_i^{\rm sop}$ are reactive power boundaries of VSC at node i. It should be noted that (14)–(16) are also hold for node $j|(i,j) \in \Omega_{\rm S}$.

3) Constraints of the OLTC: The equivalent model of an OLTC is depicted in the left side of Fig. 3. The optimization variables of the OLTC is considered as the action series of its tap steps (which is represented as $O_{t,ij}$). Considering this, the operation constraints of the OLTC are formulated as follows.

$$U_{t,j} = (o_{ij,0} + O_{t,ij}\Delta o_{ij})U_{t,i}; \tag{17}$$

$$\sum\nolimits_{t=1}^{N_T} \left|O_{t,ij} - O_{t-1,ij}\right| \le \overline{\Delta}^{\rm OLTC}; \tag{18}$$

$$-\overline{O}_{ij} \le O_{t,ij} \le \overline{O}_{ij}. \tag{19}$$

where $o_{ij,0}$ and Δo_{ij} are the initial turn ratio and increment of the OLTC; $\overline{O}_{ij}$ is the total tap steps of the OLTC; $\overline{\Delta}^{\rm OLTC}$ is the number of allowed actions for the OLTC.

4) Transactive energy price constraints: Following boundary limitation should be kept when clearing the transactive energy prices.

$$\lambda_t^{\rm min} \le \lambda_t \le \lambda_t^{\rm max} \tag{20}$$

where $\lambda_t^{\rm min}$ and $\lambda_t^{\rm max}$ are the boundaries of clearing price at period t.

B. Optimization Model of Microgrids

The optimization model of microgrids is responsible for managing the consumption plans of load demands and the usage of ESS in the transactive market organized by the DN, to minimize its operational cost that includes the interactive cost with DN, equivalent cost of inconvenience caused by DR program, and degradation cost of ESSs. With this objective settings, the optimization model of individual MG n is given as below.

$$\min \mathcal{J}_n = \sum_{\forall t} \lambda_t P_{t,n}^{\rm net}\Delta t + \sum_{\forall t}\sum_{i\in\mathcal{S}_n} \vartheta_n^{\rm Disc}(P_{t,i}^{\rm L,do} + P_{t,i}^{\rm L,up})\Delta t$$
$$+ \sum_{\forall t}\sum_{i\in\mathcal{S}_n} \mathscr{C}_{\rm deg}(c_{t,i}^{\rm ess}\eta^{\rm ess,c} + \frac{d_{t,i}^{\rm ess}}{\eta^{\rm ess,d}})\Delta t. \tag{21}$$

where $\vartheta_n^{\rm Disc}$ is the inconvenience sensitivity coefficient of MG n; $P_{t,i}^{\rm L,up}/P_{t,i}^{\rm L,do}$ are the increased/decreased load demands for DR, respectively; $\eta^{\rm ess,c}$ and $\eta^{\rm ess,d}$ are the power exchange efficiencies; $\mathcal{S}_n$ represents the set of nodes included in MG n; $\mathscr{C}_{\rm deg}$ is a coefficient concerning ESS degradation in \$/MWh, which can be calculated with its capital cost, capacity, cycling numbers, and reference state of charge (SoC) [32].

1) Operation constraints of ESS: The charging/discharing power and the state of charge of ESSs must meet the following constraints to ensure their normal operation.

$$\begin{cases} 0 \le c_{t,i}^{\rm ess} \le u_{t,i}^{\rm ess} c_i^{\rm rat} \\ 0 \le d_{t,i}^{\rm ess} \le (1-u_{t,i}^{\rm ess}) d_i^{\rm rat} \end{cases} \forall t,i \tag{22}$$

$$c_{t,i}^{\rm ess} d_{t,i}^{\rm ess} = 0 \tag{23}$$

$$S_{t,i} = S_{t-1,i} + \frac{c_{t,i}^{\rm ess}\eta^{\rm ess,c} - d_{t,i}^{\rm ess}/\eta^{\rm ess,d}}{Cap_i^{\rm ess}}\Delta t,\ \forall t,i \tag{24}$$

$$S_i^{\rm min} \le S_{t,i} \le S_i^{\rm max},\ \forall t,i \tag{25}$$

$$S_{1,i} = S_{N_T,i},\ \forall i \tag{26}$$

where $S_{t,i}$ is the state of charge of ESS i at period t; $Cap_i^{\rm ess}$ is the capacity of ESS i; $c_i^{\rm rat}$ and $d_i^{\rm rat}$ are the rated charging/discharging power of ESS i; $S_i^{\rm min}$ and $S_i^{\rm max}$ are the SoC boundaries of ESS i.

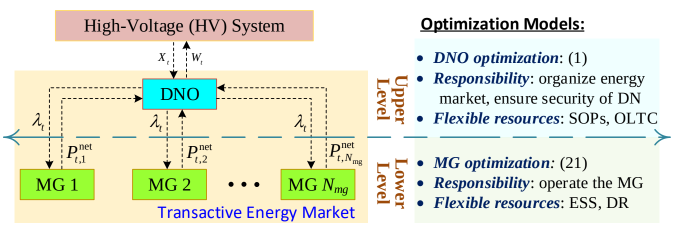

(a) Transactive control framework (b) Bilevel model

Fig. 4. (a) Transactive control framework, and (b) bilevel model for MMGs-based distribution networks.

2) Operation constraints of the demand response (DR) resources: To account for DR programs, the following operation constraints are introduced [4].

$$\begin{cases} L_{t,i}^{\rm min} \le P_{t,i}^{\rm L,up/do} \le L_{t,i}^{\rm max}, & t \in [t_i^{\rm l}, t_i^{\rm r}], \forall i \\ P_{t,i}^{\rm L,up/do} = 0, & t \notin [t_i^{\rm l}, t_i^{\rm r}], \forall i \end{cases} \tag{27}$$

$$\sum\nolimits_t P_{t,i}^{\rm L,up} = \sum\nolimits_t P_{t,i}^{\rm L,do},\ \forall i \tag{28}$$

$$P_{t,i}^{\rm L,up} P_{t,i}^{\rm L,do} = 0,\ \forall t,i \tag{29}$$

$$Q_{t,i}^{\rm L} = (P_{t,i}^{\rm L,unc} + P_{t,i}^{\rm L,up} + P_{t,i}^{\rm L,do})\tan(\cos^{-1}(pf_{\rm l})),\ \forall t,i \tag{30}$$

where $pf_{\rm l}$ is the average power factor of load demands; $P_{t,i}^{\rm L,unc}$ is the uncontrollable load demands; $Q_{t,i}^{\rm L}$ is the reactive load demands at node i at period t, respectively; $[L_{t,i}^{\rm min}, L_{t,i}^{\rm max}]$ is the range of shiftable loads; $[t_i^{\rm l}, t_i^{\rm r}]$ is the expected operation time range of shiftable loads at node i.

Although both the DNO and each microgrid are individual entities and have their own interests, by organizing a transactive energy based framework, microgrids have potential to achieve many beneficial outcomes through negotiation and coordination with DNO. Firstly, the operational power losses can be reduced through power flow optimization of the entire system. Secondly, the load consumptions can be transferred from high price periods to low price periods to reduce their electricity costs, by regulating DR and ESS. Thirdly, the local consumption of renewable power can be improved through self-management of microgrids to reduce the interactive cost with DN. In addition, the voltage security of each node in every microgrid is also ensured strictly, that benefits from the coordination optimization of DN level.

C. Transformation of the Bilevel Model

As the models formulated in Sections III-A and III-B, the combined optimization of DNO and MGs is a typical *bilevel problem* which is depicted in Fig. 4, and can be expressed as

$$\begin{aligned} &\textit{Upper Level}:\ \min\ \mathscr{F}_{\mathcal{D}}(\boldsymbol{x}); \\ &\quad \text{Subject to}: (3)-(20); \\ &\quad \text{Variables}: \boldsymbol{x} = \{\lambda_t, O_{t,ij}, P_{t,i}^{\rm sop}, Q_{t,i}^{\rm sop}\}; \\ &\qquad \lambda_t \Downarrow \quad \Uparrow P_{t,n}^{\rm net}, \forall n \\ &\textit{Lower Level}:\ \min\ \mathcal{J}_n,\ \forall n; \\ &\quad \text{Subject to}: (22)-(30); \\ &\quad \text{Variables}: P_{t,n}^{\rm net}, P_{t,i}^{\rm L,up}, P_{t,i}^{\rm L,do}, c_{t,i}^{\rm ess}, d_{t,i}^{\rm ess}. \end{aligned} \tag{31}$$

As shown in Fig. 4, the DNO optimization (1) is considered as upper level problem, whose main responsibilities are to organize transactive energy market and ensure voltage security of the distribution network by determining dynamic price λ_t and regulating SOPs and OLTC. The MG optimization (21) is regarded as lower level problem, which is responsible to operate multiple MGs to respond to the inner energy market with its flexible resources, i.e., ESS, DR. Generally, the bilevel optimization problem (31) can be solved via Stackelberg game theory [33]. As a bridge signal between DNO and MGs, the clearing price λ_t is determined by the DNO and serves as an input of the MGs' optimization problem. Based on the received λ_t, the operation of the MGs are determined by the MGs' optimization, and the power exchange between the DNO and MGs are also determined accordingly. At the same time, the power exchange must satisfy the network constraints and match the solution of the MGs' optimization. Such a method needs to obtain an equilibrium solution after an iterative process.

In order to efficiently solve the bilevel optimization problem (31), the KKT conditions of the MGs' optimization are used to transform the original bilevel optimization into a single level optimization problem. Before transforming the bilevel optimization problem, the complementary relaxation constraints of ESS and DR program need to be discussed. As [34] has proven that the nonlinear constraint (23) can be relaxed and removed from the model, and is exact for the global optimal solution, the proof is omitted here. Similarly, the complementary relaxation constraint (29) concerning the DR can also be removed safely.

On these bases, the leader-followers game problem (31) can be transformed via KKT conditions of MGs' optimization model and duality theory. (31) is thus equivalent to the follows.

$$\begin{aligned}\min \mathscr{F}_{1\mathrm{equ}} = &\{\mathbb{a}_{\mathrm{o}}(f_{\mathrm{Grid}} - \sum_t \sum_n \sum_{i\in\mathcal{S}_n} (P_{t,i}^{\mathrm{L,unc}} - P_{t,i}^{\mathrm{p}} - P_{t,i}^{\mathrm{w}})\Delta t \\ &+ f_{\mathrm{loss}} + f_{\mathrm{sw}}) + \mathbb{b}_{\mathrm{v}}\mathcal{F}_{\mathrm{vd}}\} + \sum_t \Big\{ \sum_i [\mu_{1,t,i}^{L} L_{t,i}^{\min} - \mu_{2,t,i}^{L} L_{t,i}^{\max}] \\ &+ \sum\nolimits_e (-\mu_{2,t,e}^{\mathrm{ess,c}} c_e^{\mathrm{rat}} - \mu_{2,t,e}^{\mathrm{ess,d}} d_e^{\mathrm{rat}} + \mu_{1,t,e}^{\mathrm{ess}} S_e^{\min} - \mu_{2,t,e}^{\mathrm{ess}} S_e^{\max}) \Big\}. \end{aligned} \tag{32}$$

$$\text{Subject to}: (3)-(20);$$

$$\mathbf{0} \le \boldsymbol{\mu} \perp \boldsymbol{h}(\boldsymbol{x}) \ge \mathbf{0} \ (\text{for } (22), (24)-(28), (30)) \tag{33}$$

$$\text{Variables}: \lambda_t, O_{t,ij}, P_{t,i}^{\mathrm{sop}}, Q_{t,i}^{\mathrm{sop}}, P_{t,n}^{\mathrm{net}}, P_{t,i}^{\mathrm{L,up}}, P_{t,i}^{\mathrm{L,do}}, c_{t,i}^{\mathrm{ess}}, d_{t,i}^{\mathrm{ess}}.$$

where μ and λ are the dual variables of inequality and equality constraints in optimization model of MGs, respectively. It is worth noting that the standard form (33) is available for the transitions of constraints (22), (24)-(28) and (30).

IV. Formulation of Proposed NTC Method

On the basis of above Section III, this section presents the mathematical models for slow-timescale pre-scheduling and real-time scheduling stages of the proposed NTC method to against system uncertainties, and also provides the solution methodology and implementation algorithm.

A. Uncertainty Simulation

There are a number of uncertainties from load demands and variable on-site renewables (*i.e.*, PV and WT generators) that could potentially affect the scheduling decisions of the DNO and MGs. In this work, we focus on the network-constrained transactive control between the DN and MGs, thus, prediction techniques for uncertain factors are out of scope for this paper. Therefore, a simple exponential smoothing model [35] is used to predict short-term renewable outputs and load demands $g_{t,i,r}$ based on the historical data. The active outputs of the WT generator and PV array, as well as the active load demands can be uniformly expressed as

$$g_{t,i,r} = \xi\, \overline{g}_{t,i,r} + (1-\xi)\widehat{g}_{t,i,r}, \ r = 1,2,3; \tag{34}$$

$$\widehat{g}_{t,i,r} = \overline{g}_{t,i,r}(1 + u_{i,r} \cdot \Upsilon_{i,r}). \tag{35}$$

where $r = 1,2,3$ corresponds to WT, PV, and load demands, respectively, that is $\boldsymbol{g}_{t,i,r} = [P_{t,i}^{\mathrm{w}}, P_{t,i}^{\mathrm{p}}, P_{t,i}^{\mathrm{L}}]^{\mathrm{T}}$; $\overline{g}_{t,i,r}$ and $\widehat{g}_{t,i,r}$ are the predicted value and its corresponding stochastic variable; ξ is a predetermined coefficient, such that $0 < \xi < 1$; $\Upsilon_{i,r}$ is a random number that follows specific normal distribution; $u_{i,r}$ is the uncertainty percentage of the RESs outputs or the load demands.

It remains true that the global optimal decision-making of any scheduling is made on the basis of prediction information. In this regard, the outputs of optimization problem (32) will deviated from expected ones due to the always existed prediction errors caused by the inherent uncertainties of RESs and load demands. As shown in Fig. 1, the prediction error increases with the time distance from the prediction point increases. Meanwhile, the RES power and load demands change frequently even within an hour because of their strong volatility and intermittency. These facts create the exact needs of a multi-timescale NTC architecture for an MMGs-based DN to against the system uncertainties in a dynamic manner.

B. Two-Timescale NTC Model

The proposed NTC method will be modeled from following two sub-models with different timescales, in which both sub-models are derived from Eq. (32) (which is equivalent to the bilevel model (31)) with the revisions on time interval and optimization horizon.

1) Slow-Timescale Pre-Scheduling Model

The pre-scheduling optimization stage of the NTC method is conducted in slow-timescale in a dynamic manner to provide pre-scheduling strategies from the perspective of global optimization in long time horizon, which can provide reference strategy and long-view guidance for the real-time scheduling stage [1]. In this regard, at every period t, the slow-timescale pre-scheduling model can be formulated in the following.

$$\begin{aligned} \min \ \mathscr{F}_{1\mathrm{equ}}\big|_{\Delta t}^{t\to N_T}; \\ \text{Subject to}: (3)-(20), \ (33); \end{aligned} \tag{36}$$

where symbol $\diamond\big|_{\Delta t}^{t\to N_T}$ means that the terms in (36) (the details can be seen in (2) and (32)) are calculated with period Δt from period t to N_T.

2) Real-Time Corrective Scheduling Model

To further work against the time-variant and uncertain features of the renewable energy generations and load demands, the real-time scheduling stage is designed nesting the previous stage. With the purpose of improving the control precision and implementary efficiency, this stage is conduced in fast-timescale via a rolling receding manner. In particular, the time interval Δt is divided into ζ shorter sampling periods with an interval of $\Delta\kappa$, so the t-th $\Delta t \equiv \{(t-1)\zeta + 1, \ldots, t\zeta\}\Delta\kappa$. Assuming the real-time scheduling stage is implemented in a short time horizon with $T\Delta t$, that is $\boldsymbol{T}_{\mathbf{hor}} = \{(t-1)\zeta + 1, \ldots, (t+T-1)\zeta\}$. At each time period t, based on the short-term predictions of the upcoming load demand and generations in $\boldsymbol{T}_{\mathbf{hor}}$, the real-time scheduling optimization is formulated to determine the real-time scheduling decisions for horizon

$\boldsymbol{T}_{\mathbf{hor}}$, but only the decisions at current period t is actually implemented on the distribution network.

Therefore, the real-time scheduling model is formulated as

$$\min\ \mathscr{F}_{1\text{equ}}\big|_{\Delta\kappa}^{(t-1)\zeta+1\rightarrow(t+T-1)\zeta}; \tag{37}$$

$$\text{Subject to}: (3)-(20),\ (33);$$

$$S_{(t+T-1)\zeta,e}\big|_{\Delta\kappa} = S_{(t+T-1),e}\big|_{\Delta t},\ \forall e \tag{38}$$

$$\sum_{h\in\boldsymbol{T}_{\mathbf{hor}}}(P_{h,i}^{\text{L,up}} - P_{h,i}^{\text{L,do}})\Delta\kappa = \sum_{t=t}^{t+T-1}(P_{t,i}^{\text{L,up}} - P_{t,i}^{\text{L,do}})\Delta t,\ \forall i \tag{39}$$

Similar to (36), real-time scheduling model (37) is also derived from (32), the changes are replacing Δt with $\Delta\kappa$, and the optimization horizon with $[(t-1)\zeta+1,(t+T-1)\zeta]$. Constraints (38) and (39) are used to ensure the satisfactions of (26) and (28) to balance the SoC of ESSs and satisfy the electricity consumption requirement of loads, respectively.

C. Solution Methodology and Implementation

In (36) and (37), there are many nonlinear terms in both objectives and constraints, which make the optimization problems difficult to solve. To tackle this, the following measures are adopted to convert these single-level problems into mixed integer second order cone programming problems, thus the converted problem can be efficiently solved by available off-the-shelf solvers.

1) Linearization.

Since the complementary relaxation constraints in (33) are nonlinear, the Boolean variable $\boldsymbol{\kappa}$ is introduced to transform them into linear inequality with the form of big-M constraint.

$$\mathbf{0} \le \boldsymbol{\mu} \le \boldsymbol{M\kappa} \tag{40}$$

$$\mathbf{0} \le \boldsymbol{h(x)} \le \boldsymbol{M(I-\kappa)} \tag{41}$$

where M is a large enough positive multiplier denoting the bounds of variables.

Besides the complementary relaxation constraints, variable substitution is utilized to realize the linearization of *quadratic terms*, i.e., substituting $I_{t,ij}^2$ and $U_{t,i}^2$ with $l_{t,ij}$ and $v_{t,i}$, respectively. Doing this, Eqs. (3)–(5), (11) and (12) can be transformed to linear constraints via variable substitution.

As for the nonlinear voltage deviation term in (2), auxiliary variable $Aux_{t,i}$ is introduced to express the extent of voltage deviation. The voltage deviation term can be thus linearized as:

$$\mathcal{F}_{\text{vd}} = \sum_{t=1}^{N_T}\sum_{i=1}^{N_N} Aux_{t,i} \tag{42}$$

$$Aux_{t,i} \ge v_{t,i} - \widetilde{U}_{\text{ref}}^2; Aux_{t,i} \ge \widetilde{U}_{\text{ref}}^2 - v_{t,i}; Aux_{t,i} \ge 0$$

Similarly, the tap adjusting cost of the OLTC f_{sw} can be linearized by introducing auxiliary variables $O_{t,ij}^+$ and $O_{t,ij}^-$, representing the positive/negative changes in the tap steps of the OLTC, respectively. In doing so, the cost calculation and operation constraints of the OLTC are rewritten as:

$$f_{\text{sw}} = \sum_{ij\in\Omega_O}\sum_{t=1}^{N_T}(O_{t,ij}^+ + O_{t,ij}^-); \tag{43}$$

$$\sum\nolimits_{t=1}^{N_T}(O_{t,ij}^+ + O_{t,ij}^-) \le \overline{\Delta}^{\text{OLTC}};$$

$$O_{t,ij}^+ \ge 0;\quad O_{t,ij}^- \ge 0.$$

After the variable substitution of $v_{t,i}$, constraint (17) can be re-expressed and transformed as follows.

$$v_{t,j} = v_{t,i}(1 + O_{t,ij}\Delta o_{ij})^2,\ \forall t \tag{44}$$

$$O_{t,ij} = \sum\nolimits_{x=0}^{2\overline{O}_{ij}}(x - \overline{O}_{ij})\delta_{t,ij,k},\ \delta_{t,ij,x} \in \{0,1\} \tag{45}$$

$$\sum\nolimits_{x=0}^{2\overline{O}_{ij}}\delta_{t,ij,x} = 1 \tag{46}$$

where $\delta_{t,ij,x}$ is a binary variable to represent integer variable $O_{t,ij}$. Furthermore, on the basis of (44) and (43), we now have

$$v_{t,j} = \sum\nolimits_{x=0}^{2\overline{O}_{ij}}[(o_{ij,0} + (x - \overline{O}_{ij})\Delta o_{ij})^2 v_{t,ij,x}] \tag{47}$$

$$\underline{U}^2\delta_{t,ij,x} \le v_{t,ij,x} \le \overline{U}^2\delta_{t,ij,x} \tag{48}$$

$$\underline{U}^2(1-\delta_{t,ij,x}) \le v_{t,j} - v_{t,ij,x} \le \overline{U}^2(1-\delta_{t,ij,x}) \tag{49}$$

where $v_{t,ij,x}$ is a auxiliary voltage variable to represent the nonlinear product of $v_{t,j}v_{t,ij,x}$.

2) Conic Relaxation.

To quadratic cone constraints: Using convex relaxation, Eq. (6) can be conversed to a quadratic cone constraint.

$$\left\|\begin{matrix} 2P_{t,ij} \\ 2Q_{t,ij} \\ l_{t,ij} - v_{t,i} \end{matrix}\right\|_2 \le l_{t,ij} + v_{t,i},\ \forall t \tag{50}$$

To rotated cone constraints: Similarly, Eqs. (14), (16) and (10) can be conversed to rotated quadratic cone constraints.

$$(P_{t,i}^{\text{sop}})^2 + (Q_{t,i}^{\text{sop}})^2 \le 2\frac{P_{t,i}^{\text{sop,loss}}}{\sqrt{2}A_i^{\text{sop}}}\frac{P_{t,i}^{\text{sop,loss}}}{\sqrt{2}A_i^{\text{sop}}} \tag{51}$$

$$(P_{t,i}^{alt})^2 + (Q_{t,i}^{alt})^2 \le 2\frac{S_i^{alt}}{\sqrt{2}}\frac{S_i^{alt}}{\sqrt{2}},\ alt \in \{\text{sop, p, w}\} \tag{52}$$

Through above transformation processes, i.e., linearizations and conic relaxation, the formulated non-linear programming problems (36) and (37) are transformed into MISOCP models, which can be efficiently solved using available optimization packages, such as Gurobi and CPLEX solvers.

Following the details mentioned above, the real-time control decisions of controllable resources in the DN and each MG can be determined using the proposed NTC method, which are implemented by *Algorithm 1*.

Remark 1: In this work, a SOP-based network-constrained transactive control framework is proposed to ensure the secure-economic operation of an MMGs-based distribution network. Moreover, we provide an efficient way for coordinating different financial entities, which can improve the DNO-microgrid cooperation degree, and mitigate the multiple system uncertainties. Our main feature is the introduction of SOPs, which can integrate with the AC optimal power flow technique to improve economic benefits for MGs and meanwhile ensure the voltage security and reduce the power losses of the DN. Compared to existing methods, the novelties of proposed CRSR method are summarized as follows.

1) It is secure-economic, since the new power-electronics device (i.e., SOP) can help to adjust system voltage and can actively change the system power flow, so as to regulate the transactive energy market. To our knowledge, this is the first work exploring the benefits of SOPs in transactive energy control between the MMGs and DNO.

2) It is applicable to be performed in actual MMGs-based distribution network, since it provides a complete management system from framework design, model formulation and transformation to solution technique support.

Algorithm 1 Implementation Algorithm of Proposed NTC

1: Initial parameters.
2: Formulate leader-followers transactive market between DNO and MGs according to (31).
3: Transform (31) to single level problem (32) via KKT conditions and duality.
Start to implement two-timescale NTC method in the following.
◇ *Slow-Timescale Pre-Scheduling Model*:
4: **for** $t = 1 : N_{\mathrm{T}}$ **do**
5: Collect & predict related information for $\{t, t+1, N_T\}$.
6: Formulate optimization problem (36).
7: Execute problem transformation on problem (36).
8: Solve, and deliver the results to *real-time scheduling stage*.
◇ *Real-Time Scheduling Model*:
9: **while** $h \in [(t-1)\zeta,\ t\zeta]$ **do**
10: Collect & short-term predict related information for $\boldsymbol{T}_{\mathbf{hor}}$.
11: Formulate optimization problem (37).
12: Execute problem transformation on problem (37).
13: Once the solution is obtained, implement only the actions associated with the current period h to the physical system.
14: $h \leftarrow h + 1$.
15: **end while**
16: $t \leftarrow t + 1$.
17: **end for**
◇ *Problem Transformations to MISOCP* (lines 18-21):
18: Linearize objective function through variable substitution and absolute term elimination.
19: Transform constraints into linear or conic constraints.
20: MISOCP problem is thus re-formulated from original problem.
21: **Output:** real-time scheduling strategies for OLTC, SOPs, ESSs and DR activities.

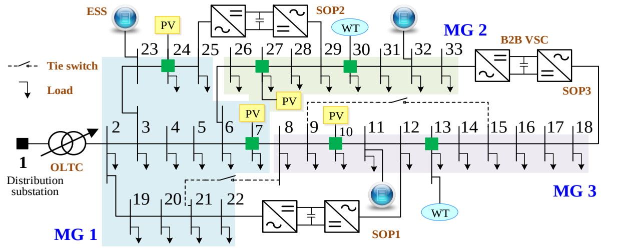

Fig. 5. Topology diagram of the modified IEEE 33-bus test system with three microgrids and three SOPs.

V. Simulation Studies

Simulations on a modified IEEE 33-bus system with three MGs and a modified IEEE 123-bus system with three MGs are performed to verify the effectiveness and correctness of the proposed network-constrained transactive control method.

A. Simulation Setups

1) Network Model: A modified IEEE 33-bus test system with three microgrids is used to validate the effectiveness of our proposed NTC method, as shown in Fig. 5. The system is consisted of 3 MGs and each pair of them is connected by a SOP, in which four PV panels and two WT generators are further installed following [29]. Moreover, an OLTC and three ESSs are additionally integrated, and their corresponding placements and parameters are shown in Table II. The other parameters are set as the standard IEEE 33-bus system.

2) Scheduling Parameter Settings: The time intervals of two timescales are 1 hour and 1/4 hour, respectively. The capacity of the installed SOPs is set as 1.0 MVA. The percentage of demands that participates the DR program is assumed to be 20% [4], [36]. The prices that the DN buys electricity from the HV system are set as Ref. [37], and the selling price of the DN is set as 0.0584 $/kWh. All the installed renewable generators

TABLE II
MODIFICATIONS IN IEEE 33-BUS TEST SYSTEM

Entity	Device	Location	Parameter
MG 1	PV unit	Buses 7, 24	650kW, 400kW
	Energy storage	Bus 6	1.0MWh, 0.2MW, 0.95
MG 2	PV unit	Bus 27	500kW
	WT unit	Bus 30	1600kW
	Energy storage	Bus 32	1.0MWh, 0.2MW, 0.95
MG 3	PV unit	Bus 10	650kW
	WT unit	Bus 13	1300kW
	Energy storage	Bus 16	1.0MWh, 0.2MW, 0.95
DN	SOPs	Buses 12-22, 25-29, 18-33	Capacity: 1.0MVA; Control mode: PQ-$V_{\mathrm{dc}}Q$
	OLTC	Buses 1-2	$\pm 5 \times 1\%$ (include $0 \times 1\%$)

TABLE III
PARAMETERS SETTINGS

Parameter	Value	Parameter	Value	Parameter	Value
Δt	1 hour	$\Delta\kappa$	1/4 hour	$\overline{\Delta}^{\mathrm{OLTC}}$	4 times/day
$\mathbb{a}_{\mathrm{o}}$	0.833	$\mathbb{b}_{\mathrm{v}}$	0.167 [29]	$\overline{U}$	1.05 p.u.
$\mathscr{C}_{\mathrm{loss}}$	Same as X_t	$\mathscr{C}_{\mathrm{deg}}$	2.736 $/MWh	$\underline{U}$	0.95 p.u.
$o_{ij,0}$	1.0	Δo_{ij}	1%	$\widetilde{U}_{\mathrm{ref}}$	1.0 p.u.
λ_t^{min}	$0.8X_t$	λ_t^{max}	$1.2X_t$	T	3 hours

are operated at a unit power factor without considering the localized reactive power support of renewables [19]. Other scheduling parameter settings are given in Table III.

3) Simulation Environment: All the simulations are conducted in the MATLAB 2018b in a 64-bit Windows environment with Gurobi 9.0 solver and YALMIP toolbox, on a PC with Core i7-8700 CPU @3.2 GHz processor and 8 GB RAM.

B. Results and Analysis

This part aims to verify the reasonability of the proposed NTC method from the respects of transactive control results, statistical performance and voltage magnitude profile.

1) Transactive control results of controllable resources. By implementing the NTC method on the modified IEEE 33-bus test system with previous setups, the obtained transactive control results concerning the active/reactive power of SOPs, charging/discharging power of ESSs, DR activities and tap positions of OLTC are shown in Fig. 6. Fig. 6(a) & 6(b) show the injected and extracted power of two sides of SOPs connected to the system, respectively. The excessive abundant power of RESs can be transfer to other MGs in need of energy supply through SOPs. The reactive power transferred through SOPs can help support the voltage profile in the end of the distribution line and thus help decrease voltage deviation. The ESS and DR can adjust the user energy consumption profile in accordance with the clearing price, which can realize peak-shaving and valley-filling to smooth the net power consumption profile. The OLTC can ensure the voltage security of the DN by regulating the tap of the transformer. The transactive energy price profile between the DNO and MGs is given in Fig. 7, acting as the price signal for the MGs to adjust their net power profiles to achieve better supply-demand balance considering the uncertainty of RESs and load demands.

2) Performance analysis. Numerical performances of the test 33-bus system under different optimization situations are listed in Table IV. From the results in Figs. 6-7 and Table IV, we can see that, the ESSs discharge and flexible loads reduce consumption during the renewable power shortage periods such as 7:00-10:00 and 14:00-20:00, and quite the contrary during the renewable power is abundant (*i.e.*, 00:00-5:00 and 11:00-14:00), thus contributing to improving the local supply-demand balance. Moreover, SOPs cooperate with the OLTC to timely respond the voltage volatility caused by RESs, which can effectively lower the security risks of the DN operation. With accurately power flow regulating ability, the SOPs are

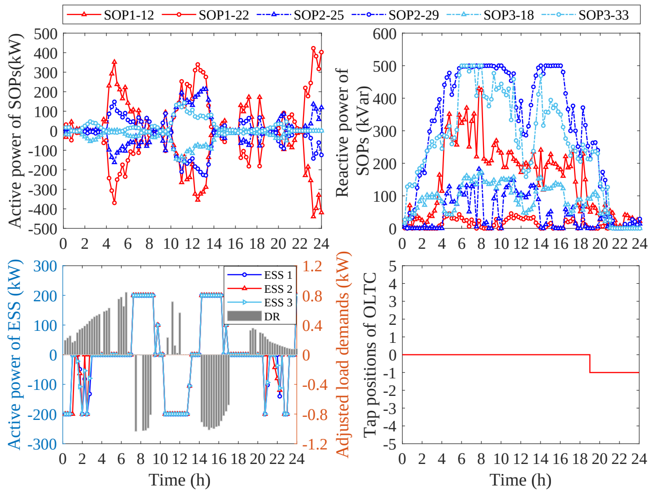

Fig. 6. Final transactive control results: (a)-(b) active and reactive power of the three SOPs; (c) control strategies of ESSs and DR activities; (d) optimal tap positions of the OLTC.

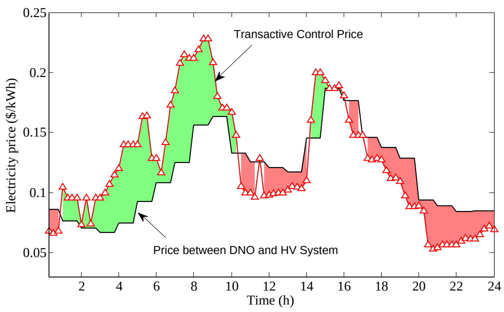

Fig. 7. Transactive energy price curve between the DNO and the MGs.

TABLE IV
PERFORMANCES DATA OF THE MMGS-BASED DISTRIBUTION NETWORK

System performance	Unscheduling mode[1]	Proposed NTC method: Pre-Scheduling	Proposed NTC method: Real-time Scheduling	Ideal mode[2]
Line power losses (kWh)	1736.04	756.86	749.82	718.62
SOP power losses (kWh)	0	502.50	509.97	518.39
Voltage deviation (p.u.^{2}) (calculated by $\mathcal{F}_{\mathrm{vd}}$ in (2))	22.86	18.00	13.57	12.96
Profit of DNO ($)	430.28	635.176	753.907	790.53
Total cost of MGs ($)	5536.96	5324.08	5045.86	4825.85

[1]For the unscheduling mode, it simulates the passive operation of the test system, where the optimal control of the flexible resources belonging to the DNO and MGs is not implemented (a reference case). Herein, the voltage limits are removed to avoid an unacceptably huge amount of load shedding and renewable curtailment [1].

[2]For the ideal mode, it is assumed that all the needed information are known to DNO in advance with perfect predictions.

able to greatly reduce the line losses and voltage deviations of DN systems compared to the unscheduling mode.

Also, it is straightforward from Table IV that with smaller timescale, higher accuracy and better results are achieved in real-time scheduling. The reason lies in the fact that the final control strategies are obtained via a dynamic updated manner in smaller scheduling granularity based on the latest updated information, which has proved to be efficient enough to against system uncertainties.

3) Voltage profile. System voltage magnitude is an important indicator to represent the operational security of DNs. The voltage profiles of all the 33 nodes over real-time scheduling are shown in Fig. 8. Obviously, the proposed NTC can eliminate all voltage violations by adjusting system power flow via SOPs, thus strictly maintaining the voltage magnitudes within safety range (*i.e.*, [0.95, 1.05] p.u.). As such, the security of the DN operation can be ensured. Moreover, compared to the unscheduling mode, the voltage deviation performed by the NTC method is reduced by 43.30%, which could mitigate the

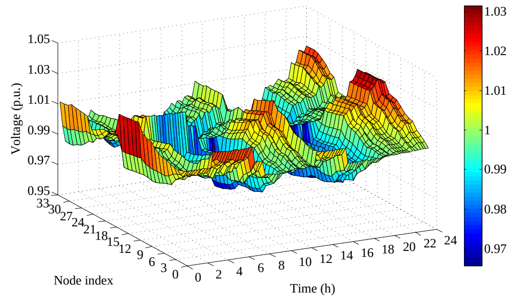

Fig. 8. Voltage profiles of all 33 nodes over an operational day.

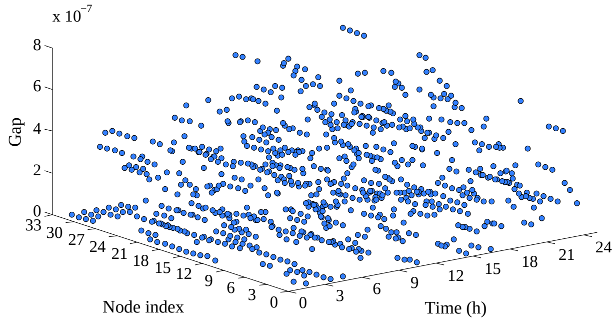

Fig. 9. Gap values at each node over the scheduling horizon.

adverse effects of the uncertainties on system security.

4) Verification of solution accuracy. The inequality constraint (50) is relaxed from equality (6), thus the relaxation error (also referred as relaxation gap value) is calculated as (53) to estimate the accuracy of the conic relaxation.

$$Gap_t = \max \left| l_{t,ij} - \frac{P_{t,ij}^2 + Q_{t,ij}^2}{v_{t,i}} \right|, \ \forall t \tag{53}$$

The gap values of the proposed method at each node over the scheduling horizon are depicted in Fig. 9. It is obvious that the gap values at every time period are all at a 10^{-7} level, which are regarded to be small enough. That is to say, the second-order convex relaxation has quite acceptable accuracy for our formulated problem.

According to above analyses, the proposed NTC method employs the SOPs as an active measure in DN-level for supplementing the transactive market between DNO and MMGs, which is proved to be of great ability to eliminate voltage violations and decrease power losses, thus effectively improving the operational security and economy of DNs simultaneously.

C. Sensitive Analysis Towards Uncertainties

In reality, the predictions are always not perfect due to the inherent intermittency and volatility of RESs [20]. Therefore, in order to verify the robustness of our proposed NTC method for working against uncertainties, a sensitive analysis under various uncertainty settings is performed in this part. Consequently, Table V lists the test results under different uncertainty levels of prediction errors, and Fig. 10 shows the improved performances of real-time scheduling stage with comparison of slow-timescale stage in three test scenarios.

From the results we can know that, with the increasing levels of prediction errors, the various performances of unscheduling model consistently become worse. Also, Fig. 10 shows that the improved performances in terms of DNO profit, total MGs cost and voltage deviation are more visible with the ascending levels of prediction errors, but the gap from the ideal mode is still constantly widening.

TABLE VI
PERFORMANCE COMPARISON AMONG THE FIVE CASES

System performance	Unscheduling mode	Case I	Case II	Case III	Case IV (proposed NTC method)
Line power losses (kWh)	2056.486	908.736	819.074	1942.462	769.327
SOP power losses (kWh)	0	632.962	545.477	0	526.263
Voltage deviation (p.u.^{2})	23.460	89.471	15.860	23.381	14.228
Profit of DNO ($)	418.821	830.446	1353.810	802.722	919.325
Total cost of MGs ($)	5219.757	4973.600	5421.541	5093.116	5018.813

TABLE V
PERFORMANCE COMPARISON OF NTC METHOD UNDER DIFFERENT UNCERTAINTY LEVELS

Unc. Scena.	Performances	Deterministic mode[1]	Proposed NTC method Pre-Scheduling	Proposed NTC method Real-time Scheduling	Ideal mode
1	Power losses (kWh)	919.63	756.86	749.82	718.62
	Profit of DNO ($)	554.18	635.176	753.907	790.53
	Tot. cost of MGs ($)	5425.31	5324.08	5045.86	4825.85
	Volt. dev. (p.u.^{2})	20.24	18.00	13.57	12.96
2	Power losses (kWh)	927.38	765.08	754.37	709.10
	Profit of DNO ($)	556.90	589.608	750.131	801.81
	Tot. cost of MGs ($)	5422.32	5372.43	5049.79	4746.80
	Volt. dev. (p.u.^{2})	20.37	18.17	13.64	12.80
3	Power losses (kWh)	933.56	746.56	722.90	663.91
	Profit of DNO ($)	452.81	456.335	934.126	1024.64
	Tot. cost of MGs ($)	5388.19	5365.17	5011.11	4612.23
	Volt. dev. (p.u.^{2})	20.39	18.68	13.32	12.25

[1] A deterministic NTC formulation using predicted information for decision-making without considering uncertainties.

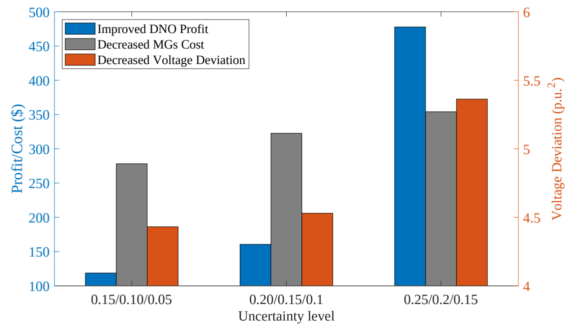

Fig. 10. The improved performances of real-time scheduling stage. (Note: the uncertainty level $a/b/c$ means that uncertainties $u_{i,r}$ [4] of WT, PV, and load demands are set as a, b and c, respectively.)

These facts indicate that the prediction uncertainties concerning renewables and consumptions will have adverse effects on the economic and secure performances of the DN system, and this kind of adverse effects increase with the prediction error increases. Furthermore, compared to unscheduling and single-layer models, the robustness of the proposed two-timescale NTC method is verified as it can indeed mitigate the adverse effects of the uncertainties through dynamic double-layer strategies updating, and it shows more potential in cost savings and voltage regulation as uncertainties grow larger.

D. Case studies

In this subsection, we tend to validate the effectiveness of the proposed NTC method and examine the effect of each salient feature through case studies. For this purpose, four typical cases are further conducted and compared, which are defined as follows. Specifically, we randomly choose a set of scenarios under uncertainty level of $0.25/0.2/0.15$ for test.

Case I: Economy-oriented transactive control. In this case, only economy-concerned factors are considered in the transactive control framework, thus the power flow, line power losses and voltage deviation are not included.

Case II: Network-constrained non-market-based control. In this case, the trading price between the DNO and MGs is the HV grid price multiplied by a number greater than 1 (i.e., 1.2). That is, the transactive energy market is not considered.

Case III: Network-constrained transactive control without considering the active measure of optimal controlling SOPs.

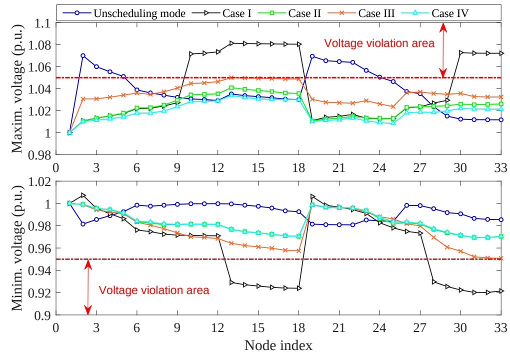

Fig. 11. Extreme voltage magnitude comparisons of the 5 cases. (a) Maximum voltage profiles; (b) Minimum voltage profiles in each node.

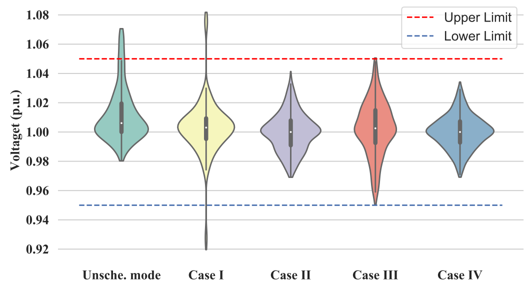

Fig. 12. Voltage magnitude distributions in *Violin plot* for 5 cases.

Case IV: The proposed NTC method in previous sections.

With above definitions, the comparison results of five cases (including unscheduling mode) are listed in Table VI. Their extreme voltage magnitude comparisons and voltage magnitude distributions in violin plot are shown in Fig. 11 and Fig. 12, respectively.

From the results, it can be seen that our proposed NTC method performs better than other four cases in both economy and security aspects. Case I is an economy-oriented method, and thus results in a lower MGs cost due to the fully utilization of ESS and DR without considering the violations of network constraints. We further conduct power lower calculation for it using its obtained strategies, the results show that it has larger line losses and voltage deviation in comparison with Case IV, and raises voltage violations as depicted in Fig. 12. In Case II, drooping transactive energy market results in uneven distribution of benefits between DNO and MGs. In this case, the ESS and DR action less, so the SOPs in DN-level make more efforts for power flow regulation, thus leading to larger SOP power losses. In Case III, after removing SOPs, the line losses and voltage deviation are increased by 152.49% and 64.33% respectively compared to Case IV, which precisely verifies the benefits of SOPs in reshaping system power flow to deal with security issues of DNs.

In summary, we can conclude from above analyses that the proposed NTC method is able to actively optimize the secure operation of the MMGs-based DN system besides providing a platform to coordinate the DNO and MGs with respectation of their interests, through innovatively integrate a transactive energy market with the novel power-electronics device SOP-based power flow regulation technique. Although a fraction of economy is sacrificed, the security of entire system operation

This article has been accepted for publication in IEEE Transactions on Sustainable Energy. This is the author's version which has not been fully edited and content may change prior to final publication. Citation information: DOI 10.1109/TSTE.2023.3246360

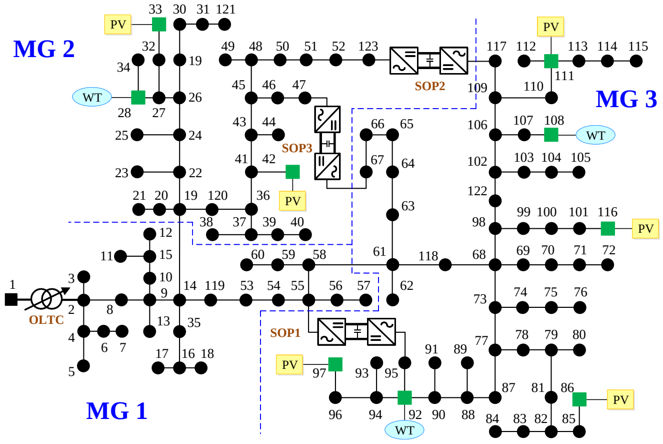

Fig. 13. Topology diagram of the modified IEEE 123-bus test system with 3 microgrids and 3 SOPs.

TABLE VII
STATISTICAL DATA OF THE 123-BUS TEST SYSTEM PERFORMANCES

System Performances	Unscheduling method	Proposed NTC method	
		24 periods	96 periods
Line power losses (kWh)	2511.5512	1230.3130	1218.4124
SOP power losses (kWh)	0	631.1488	532.6454
Voltage deviation (p.u.^{2})	58.0480	24.4436	20.4614
Profit of DNO ($)	547.6136	1063.0895	1176.6309
Total cost of MGs ($)	6323.9590	5847.1102	5753.6463

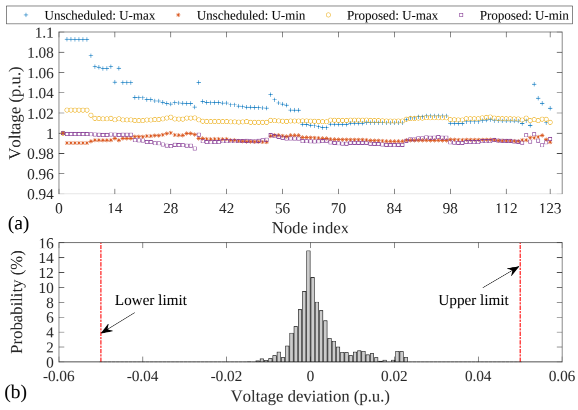

Fig. 14. (a) Extreme voltage magnitudes of the modified IEEE 123-bus system in proposed and unscheduling modes. (b) Distribution of voltage deviations achieved by our proposed method.

can be thus absolutely guaranteed.

E. Test on The Large System

In this part, a modified IEEE 123-bus test system is simulated to verify the scalability of the proposed method. As is shown in Fig. 13 [38], the test system is composed of 3 networked microgrids which are equipped with 6 PV arrays and 3 WTs and while on the grid side, an OLTC and 3 SOPs are installed to improve the performance of the distribution system. The PV arrays are installed on nodes 33, 42, 86, 97, 111 and 116 with capacities of 600kWh, 300kWh, 500kWh, 400kWh, 500kWh and 500kWh respectively, and the WTs are installed on nodes 28, 92 and 108 all with capacity of 1200kWh. The parameter value settings of enormous controllable devices are exactly the same as Section V-A. The test results are shown in Table VII which contains each item of costs and voltage deviation of unscheduling and proposed methods respectively. Fig. 14 presents the extreme voltage magnitudes of the test system and distribution of voltage deviations achieved by the proposed NTC method.

TABLE VIII
ANALYSIS OF COMPUTATIONAL PERFORMANCES OVER MODEL COMPLEXITY AND COMPUTATIONAL TIME COST

Test system	Model complexity		Computational time cost (s)		
	Number of		Problem formulation	Optimization solving	Total time cost
	Constraint	Variable			
33-bus	10453	8808	24.03	191.46	239.57
	6217	5638	7.42	6.48	22.16
123-bus	36520	28252	81.33	506.58	638.06
	22458	18499	52.20	45.07	129.64

As is depicted by the comparison with the unscheduling method in obtained results, the power losses and voltage deviations of the proposed NTC method have been reduced by 30.28% and 64.75%, respectively, and the total operational utility of the entire distribution system has been improved by 20.76%. The comparison has proved that the proposed method can achieve a quite satisfying performance and scalability in the large-scale system both in economic and voltage security aspects, such as system operational utility improvement, power losses reduction, and voltage deviation mitigation. In conclusion, our proposed NTC method can be applied widely to different distribution networks and maintain good performances at the same time.

F. Analysis of the Practical Feasibility

Computational performance. To analyze the computational performances of the proposed NTC method, the model complexity and computational time cost of our proposed NTC method under two test systems are calculated and tested. The proposed algorithm and simulation are implemented in the MATLAB 2018b equipped with Gurobi optimization solver and YALMIP toolbox. A detailed report of computational performances is summarized in Table VIII.

Generally, when solving the formulated model using off-the-shelf solvers, the total computational time cost is composed of time for problem formulation, optimization solving, and other time used for constraint processing and assignment [39]. From the results in Table VIII, we see that the solving of the pre-scheduling stage is a little time-consuming due to the quite high model complexity, but it can also be finished in several minutes. This is acceptable since this stage is solved ahead of actual schedules, thus the requirement on the computation time is not very strict. For the real-time corrective scheduling, the main computation time is spent in the model formulation term, and it can be solved within a short time in both two test systems. Due to the binary parameter introduced by the KKT complementary condition, it's inevitible to increase the model complexity as the scale of the system becomes larger, but the algorithm optimization solving time doesn't increase significantly. More computational efficient techniques can be further incorporated. From the above results, a conclusion can be drawn that the proposed algorithm has an acceptable computation efficiency within tolerance in applications of the large-scale distribution system.

VI. CONCLUSION

In this paper, we propose a network-constrained transactive control framework for an MMGs-based distribution network considering uncertainties. Different from previous TC studies, this framework can not only address the economic issues of transactive market between the DNO and the MGs, but also can adjust DN operation by optimally regulating the OLTC and the novel power-electronics device (i.e., SOPs). In this way, economic and technical issues are thus addressed in a holistic manner. In particular, we innovatively integrate a collaborative optimization mechanism with the OPF technique. A dynamic two-timescale model is formulated to minimize operational cost, improve voltage profile and against adverse effects of uncertainties. Case studies on a modified IEEE 33-bus distribution feeder with three MGs demonstrate the effectiveness of our proposed NTC method and algorithm.

References

[1] X. Yang, C. Xu, H. He, W. Yao, J. Wen, and Y. Zhang, "Flexibility provisions in active distribution networks with uncertainties," *IEEE Trans. Sustain. Energy*, vol. 12, no. 1, pp. 553–567, 2021.

[2] X. Xue, X. Ai, J. Fang, S. Cui, Y. Jiang, W. Yao, Z. Chen, and J. Wen, "Real-time schedule of microgrid for maximizing battery energy storage utilization," *IEEE Trans. Sustain. Energy*, vol. 13, no. 3, pp. 1356–1369, 2022.

[3] H. Qiu, W. Gu, Y. Xu, Z. Wu, S. Zhou, and G. Pan, "Robustly multi-microgrid scheduling: Stakeholder-parallelizing distributed optimization," *IEEE Trans. Sustain. Energy*, vol. 11, no. 2, pp. 988–1001, 2020.

[4] X. Yang, H. He, Y. Zhang, Y. Chen, and G. Weng, "Interactive energy management for enhancing power balances in multi-microgrids," *IEEE Trans. Smart Grid*, vol. 10, no. 6, pp. 6055–6069, 2019.

[5] F. Lezama, J. Soares, P. Hernandez-Leal, M. Kaisers, T. Pinto, and Z. Vale, "Local energy markets: Paving the path toward fully transactive energy systems," *IEEE Trans. Power Syst.*, vol. 34, no. 5, pp. 4081–4088, 2019.

[6] S. Cui, Y. W. Wang, Y. Shi, and J. W. Xiao, "An efficient peer-to-peer energy-sharing framework for numerous community prosumers," *IEEE Trans. Ind. Informat.*, vol. 16, no. 12, pp. 7402–7412, 2020.

[7] B. Papari, C. S. Edrington, M. Ghadamyari, M. Ansari, G. Ozkan, and B. Chowdhury, "Metrics analysis framework of control and management system for resilient connected community microgrids," *IEEE Trans. Sustain. Energy*, vol. 13, no. 2, pp. 704–714, 2022.

[8] H. Zhang, C. Chen, S. Lei, and Z. Bie, "Resilient distribution system restoration with communication recovery by drone small cells," *IEEE Trans. Smart Grid*, 2022, to be published. DOI: 10.1109/TSG.2022.3210771.

[9] X. Mo, J. Zhu, J. Chen, Y. Guo, Y. Xia, and M. Liu, "A stochastic spatiotemporal decomposition decision-making approach for real-time dynamic energy management of multi-microgrids," *IEEE Trans. Sustain. Energy*, vol. 12, no. 2, pp. 821–833, 2021.

[10] R. Sadnan, S. Poudel, A. Dubey, and K. P. Schneider, "Layered coordination architecture for resilient restoration of power distribution systems," *IEEE Trans. Ind. Informat.*, 2022, to be published. DOI: 10.1109/TII.2022.3177464.

[11] B. Zhao, X. Wang, D. Lin, M. M. Calvin, J. C. Morgan, R. Qin, and C. Wang, "Energy management of multiple microgrids based on a system of systems architecture," *IEEE Trans. Power Syst.*, vol. 33, no. 6, pp. 6410–6421, 2018.

[12] A. M. Jadhav, N. R. Patne, and J. M. Guerrero, "A novel approach to neighborhood fair energy trading in a distribution network of multiple microgrid clusters," *IEEE Trans. Ind. Electron.*, vol. 66, no. 2, pp. 1520–1531, 2019.

[13] C. Wang, T. Tian, Z. Xu, S. Cheng, S. Liu, and R. Chen, "Optimal management for grid-connected three/single-phase hybrid multimicrogrids," *IEEE Trans. Sustain. Energy*, vol. 11, no. 3, pp. 1870–1882, 2020.

[14] Z. Zhao, J. Guo, C. S. Lai, H. Xiao, K. Zhou, and L. L. Lai, "Distributed model predictive control strategy for islands multimicrogrids based on non-cooperative game," *IEEE Trans. Ind. Informat.*, vol. 17, no. 6, pp. 3803–3814, 2021.

[15] M. M. Esfahani, A. Hariri, and O. A. Mohammed, "A multiagent-based game-theoretic and optimization approach for market operation of multimicrogrid systems," *IEEE Trans. Ind. Informat.*, vol. 15, no. 1, pp. 280–292, 2019.

[16] X. Yang, Y. Zhang, H. Wu, J. Wen, and S. Cheng, "Enabling online scheduling for multi-microgrid systems: An event-triggered approach," *IEEE Trans. Smart Grid*, vol. 12, no. 3, pp. 1836–1852, 2021.

[17] K. Anoh, S. Maharjan, A. Ikpehai, Y. Zhang, and B. Adebisi, "Energy peer-to-peer trading in virtual microgrids in smart grids: A game-theoretic approach," *IEEE Trans. Smart Grid*, vol. 11, no. 2, pp. 1264–1275, 2020.

[18] Y. Wang, Z. Huang, M. Shahidehpour, L. L. Lai, Z. Wang, and Q. Zhu, "Reconfigurable distribution network for managing transactive energy in a multi-microgrid system," *IEEE Trans. Smart Grid*, vol. 11, no. 2, pp. 1286–1295, 2020.

[19] H. Ji, C. Wang, P. Li, F. Ding, and J. Wu, "Robust operation of soft open points in active distribution networks with high penetration of photovoltaic integration," *IEEE Trans. Sustain. Energy*, vol. 10, no. 1, pp. 280–289, 2019.

[20] T. Ding, Q. Yang, Y. Yang, C. Li, Z. Bie, and F. Blaabjerg, "A data-driven stochastic reactive power optimization considering uncertainties in active distribution networks and decomposition method," *IEEE Trans. Smart Grid*, vol. 9, no. 5, pp. 4994–5004, 2018.

[21] P. Li, H. Ji, C. Wang, J. Zhao, G. Song, F. Ding, and J. Wu, "Optimal operation of soft open points in active distribution networks under three-phase unbalanced conditions," *IEEE Trans. Smart Grid*, vol. 10, no. 1, pp. 380–391, 2019.

[22] H. Saber, H. Ranjbar, S. F.-Dehkordi, M. M.-Aghtaie, M. Ehsan, and M. Shahidehpour, "Transactive energy management of V2G-capable electric vehicles in residential buildings: An MILP approach," *IEEE Trans. Sustain. Energy*, vol. 13, no. 3, pp. 1734–1743, 2022.

[23] Z. Liu, L. Wang, and L. Ma, "A transactive energy framework for coordinated energy management of networked microgrids with distributionally robust optimization," *IEEE Trans. Power Syst.*, vol. 35, no. 1, pp. 395–404, 2020.

[24] M. Yan, M. Shahidehpour, A. Paaso, L. Zhang, A. Alabdulwahab, and A. Abusorrah, "Distribution network-constrained optimization of peer-to-peer transactive energy trading among multi-microgrids," *IEEE Trans. Smart Grid*, vol. 12, no. 2, pp. 1033–1047, 2021.

[25] X. Yang, Z. Zhou, Y. Zhang, J. Liu, J. Wen, Q. Wu, and S. Cheng, "Resilience-oriented co-deployment of remote-controlled switches and soft open points in distribution networks," *IEEE Trans. Power Syst.*, 2022, to be published. DOI: 10.1109/TPWRS.2022.3176024.

[26] C. Wang, C. Sun, P. Li, J. Wu, F. Feng, and Y. Yu, "SNOP-based operation optimization and analysis of distribution networks," *Automa. Electric Power Syst.*, vol. 39, no. 9, pp. 82–87, 2015.

[27] H. Farzin, M. Fotuhi-Firuzabad, and M. Moeini-Aghtaie, "Enhancing power system resilience through hierarchical outage management in multi-microgrids," *IEEE Trans. Smart Grid*, vol. 7, no. 6, pp. 2869–2879, 2016.

[28] Y. Du and F. Li, "Intelligent multi-microgrid energy management based on deep neural network and model-free reinforcement learning," *IEEE Trans. Smart Grid*, vol. 11, no. 2, pp. 1066–1076, 2020.

[29] P. Li, H. Ji, C. Wang, J. Zhao, G. Song, F. Ding, and J. Wu, "Coordinated control method of voltage and reactive power for active distribution networks based on soft open point," *IEEE Trans. Sustain. Energy*, vol. 8, no. 4, pp. 1430–1442, 2017.

[30] A. Pouladi and A. K. Zadeh, "Fast coscheduling of discrete and continuous resources in active distribution systems," *IEEE Systems Journal*, vol. 16, no. 1, pp. 24–32, 2022.

[31] T. Zhang, X. Yu, Y. Mu, H. Jia, K. Hou, and X. Jin, "Multiple sources restoration for soft open points in distribution networks with a two-stage accelerated algorithm," *IEEE Trans. Sustain. Energy*, 2022, to be published. DOI: 10.1109/TSTE.2022.3226750.

[32] D. Xu, B. Zhou, N. Liu, Q. Wu, N. Voropai, C. Li, and E. Barakhtenko, "Peer-to-peer multienergy and communication resource trading for interconnected microgrids," *IEEE Trans. Ind. Informat.*, vol. 17, no. 4, pp. 2522–2533, 2021.

[33] M. Tavakkoli, S. Fattaheian-Dehkordi, M. Pourakbari-Kasmaei, M. Liski, and M. Lehtonen, "Bonus-based demand response using stackelberg game approach for residential end-users equipped with HVAC system," *IEEE Trans. Sustain. Energy*, vol. 12, no. 1, pp. 234–249, 2021.

[34] Z. Li, Q. Guo, H. Sun, and J. Wang, "Sufficient conditions for exact relaxation of complementarity constraints for storage-concerned economic dispatch," *IEEE Trans. Power Syst.*, vol. 31, no. 2, pp. 1653–1654, 2016.

[35] X. Yang, Y. Zhang, H. He, S. Ren, and G. Weng, "Real-time demand side management for a microgrid considering uncertainties," *IEEE Trans. Smart Grid*, vol. 10, no. 3, pp. 3401–3414, 2019.

[36] M. R. M. Cruz, D. Z. Fitiwi, S. F. Santos, S. J. P. S. Mariano, and J. P. S. Catalo, "Multi-flexibility option integration to cope with large-scale integration of renewables," *IEEE Trans. Sustain. Energy*, vol. 11, no. 1, pp. 48–60, 2020.

[37] Y. Li, C. Feng, F. Wen, K. Wang, and Y. Huang, "Energy pricing and management for park-level energy internets with electric vehicles and power-to-gas devices," *Automa. Electric Power Syst.*, vol. 42, no. 16, pp. 1–10, 2018.

[38] A. Arif, Z. Wang, C. Chen, and J. Wang, "Repair and resource scheduling in unbalanced distribution systems using neighborhood search," *IEEE Trans. Smart Grid*, vol. 11, no. 1, pp. 673–685, 2020.

[39] Y. Jiang, C. Wan, J. Wang, Y. Song, and Z. Y. Dong, "Stochastic receding horizon control of active distribution networks with distributed renewables," *IEEE Trans. Power Syst.*, vol. 34, no. 2, pp. 1325–1341, 2019.

Xiaodong Yang (S'17-M'19) received the Ph.D. degree in control science and engineering from the Zhejiang University of Technology, Hangzhou, China, in 2019.

He was a joint Ph.D. student with the Department of Electrical, Computer, and Biomedical Engineering, University of Rhode Island, Kingston, RI, USA, from 2017 to 2019. From 2019 to 2021, he was a Postdoctoral Research Fellow with the Huazhong University of Science and Technology (HUST), Wuhan, China. He is currently an Associate Professor with the School of Electrical Engineering and Automation, Hefei University of Technology, Hefei, China. His current research interests include resilient distribution system, multi-microgrids system, electric demand response, and power system control and optimization.

Zehao Song received the B.Eng. degree in electrical engineering from the Zhejiang University of Technology, Hangzhou, China, in 2018. He is now pursing the M.Eng. degree in electrical engineering in Tsinghua Berkeley Shenzhen Institute, Tsinghua University.

His research interest includes energy management of power systems and distributed optimization.

Jinyu Wen (M'10) received the B.S. and Ph.D. degrees in electrical engineering from Huazhong University of Science and Technology (HUST), Wuhan, China, in 1992 and 1998, respectively.

He was a Visiting Student from 1996 to 1997 and Research Fellow from 2002 to 2003 all at the University of Liverpool, Liverpool, UK, and a Senior Visiting Researcher at the University of Texas at Arlington, Arlington, USA, in 2010. From 1998 to 2002 he was a Director Engineer with XJ Electric Co. Ltd. in China. In 2003, he joined the HUST and now is a Professor with the School of Electrical and Electronics Engineering, HUST. His current research interests include renewable energy integration, energy storage, multi-terminal HVDC and power system operation and control.

Lijian Ding was born in China in 1970. He received the B.S. and M.Sc. degrees in electrical engineering from the Harbin Institute of Technology, Harbin, China, in 1992 and 1995, respectively, the Ph.D. degree from North China Electric Power University, Beijing, China, in 2000, and the EMBA degree from the China Europe International Business School, Shanghai, China, in 2013.

He is currently a Professor with the School of Electrical Engineering and Automation, Hefei University of Technology, Hefei, China, and also with the Institute of Energy, Hefei Comprehensive National Science Center, Hefei. His current research interests include fault state identification and diagnosis, integrated signal information processing, high voltage technology, and applications.

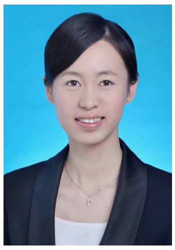

Menglin Zhang received the B.S. degree in electrical engineering and automation from Southwest Jiaotong University, Chengdu, China, in 2011, and Ph.D. degree from the Department of Electrical Engineering, Wuhan University, Wuhan, China, in 2017. She was with the Department of Electrical and Electronic Engineering, Huazhong University of Science and Technology (HUST), Wuhan, China from 2017 to 2019. She was a postdoctoral researcher with the Center for Electric Power and Energy, Technical University of Denmark (DTU) from 2019 to 2021.

Currently, she is a professor with the school of automation, China University of Geosciences, Wuhan, China. Her research includes the optimal operation of renewable-based multi-energy systems under uncertainty, including the modeling of multi-energy systems considering flexibility, robust and stochastic optimization, and the solution for bulk energy systems.

Qiuwei Wu (M'08-SM'15) obtained the B. Eng. and M. Eng. in Power System and Its Automation from Nanjing University of Science and Technology in 2000 and 2003, respectively, and the PhD degree in Power System Engineering from Nanyang Technological University, Singapore, in 2009.

He has been a tenured Associate Professor with Tsinghua-Berkeley Shenzhen Institute, Tsinghua Shenzhen International Graduate School, Tsinghua University since Jan. 2022. He was a senior R&D engineer with Vestas Technology R&D Singapore Pte Ltd from Mar. 2008 to Oct. 2009. He was working at Department of Electrical Engineering, Technical University of Denmark (DTU) from Nov. 2009 to Aug. 2021 (PostDoc Nov. 2009-Oct. 2010, Assistant Professor Nov. 2010-Aug. 2013, Associate Professor Sept. 2013-Aug. 2021). He was a visiting scholar at the Department of Industrial Engineering & Operations Research (IEOR), University of California, Berkeley, from Feb. 2012 to May 2012 funded by the Danish Agency for Science, Technology and Innovation (DASTI), Denmark. He was a visiting professor named by Y. Xue, an Academician of the Chinese Academy of Engineering, at Shandong University, China, from Nov. 2015 to Oct. 2017. He was a visiting scholar at the School of Engineering and Applied Sciences, Harvard University from Nov. 2017 – Oct. 2018 funded by the Otto Mønsted Fond. He was a visiting Associate Professor at Tsinghua-Berkeley Shenzhen Institute, Tsinghua University from Aug. 2021 to Dec. 2021.

His research interests are decentralized/distributed optimal operation and control of power systems with high penetration of renewables, including distributed wind power modelling and control, decentralized/distributed congestion management, voltage control and load restoration of active distribution networks, and decentralized/distributed optimal operation of integrated energy systems. He is an Associate Editor of IEEE Transactions on Power Systems and IEEE Power Engineering Letters. He is also the deputy editor-in-chief and an Associate Editor of International Journal of Electrical Power and Energy Systems, and Journal of Modern Power Systems and Clean Energy. He is a subject editor for IET Generation, Transmission & Distribution, and IET Renewable Power Generation.

Shijie Cheng (M'86-SM'87-F'11-LF'18) received the B.S. degree from Xi'an Jiaotong University, Xi'an, China, in 1967, the M.Sc. degree from Huazhong University of Science and Technology, Wuhan, China, in 1981, and the Ph.D. degree from the University of Calgary, Calgary, AB, Canada, in 1986, all in the electrical engineering.

He has been a Professor with the School of Electrical and Electronics Engineering, Huazhong University of Science and Technology, Wuhan, China, since 1991. His research interests are power system control, stability analysis, application of Artificial Intelligence, and energy storage.

Prof. Cheng is a Fellow of the Chinese Academy of Sciences.